

# Charge and magnetic order in the spin-one-half Falicov-Kimball model with Hund coupling in two dimensions

Hana Čenčariková, Pavol Farkašovský, Natália Tomašovičová  
and Martin Žonda

Institute of Experimental Physics, Slovak Academy of Sciences  
Watsonová 47, 040 01 Košice, Slovakia

## Abstract

The spin-one-half Falicov-Kimball model with spin-dependent on-site interaction between localized ( $f$ ) and itinerant ( $d$ ) electrons is studied by small-cluster exact-diagonalization calculations and a well-controlled approximative method in two dimensions. The results obtained are used to categorize the ground-state configurations according to common features (charge and spin ordering) for all  $f$  and  $d$  electron concentrations ( $n_f$  and  $n_d$ ) on finite square lattices. It is shown that only a few configuration types form the basic structure of the charge phase diagram in the  $n_f - n_d$  plane. In particular, the largest regions of stability correspond to the phase segregated configurations, the axial striped configurations and configurations that can be considered as mixtures of chessboard configurations and the full (empty) lattice. Since the magnetic phase diagram is much richer than the charge phase diagram, the magnetic superstructures are examined only at selected values of  $f$  and  $d$  electron concentrations.

PACS numbers.:75.10.Lp, 71.27.+a, 71.28.+d

# 1 Introduction

The interplay between charge and spin degrees of freedom in strongly correlated systems has triggered enormous interest in recent years due to the rich variety of charge and spin orderings found in some rare-earth and transition-metal compounds. Charge and spin superstructures have been observed, for example, in doped nickelate [1], cuprate [2] and cobaltate [3] materials, some of which constitute materials that exhibit high-temperature superconductivity. One of the simplest models suitable to describe charge-ordered phases in interacting electron systems is the Falicov-Kimball model (FKM) [4]. Indeed, it was shown that the simplest version of this model (the spinless FKM) already exhibits an extremely rich spectrum of charge ordered solutions, including various types of periodic, phase-separated and striped phases [5, 6]. However, the spinless version of the FKM, although nontrivial, is not able to account for all aspects of real experiments. For example, many experiments show that a charge superstructure is accompanied by a magnetic superstructure [1, 2, 7]. In order to describe both types of ordering in the unified picture, a simple model based on a generalization of the spin-one-half FKM with an anisotropic, spin-dependent interaction that couples the localized and itinerant subsystems was proposed [8]. Thus the model Hamiltonian can be written as

$$H = \sum_{ij\sigma} t_{ij} d_{i\sigma}^+ d_{j\sigma} + U \sum_{i\sigma\sigma'} f_{i\sigma}^+ f_{i\sigma} d_{i\sigma'}^+ d_{i\sigma'} + J \sum_{i\sigma} (f_{i-\sigma}^+ f_{i-\sigma} - f_{i\sigma}^+ f_{i\sigma}) d_{i\sigma}^+ d_{i\sigma} , \quad (1)$$

where  $f_{i\sigma}^+, f_{i\sigma}$  are the creation and annihilation operators for an electron of spin  $\sigma = \uparrow, \downarrow$  in the localized state at lattice site  $i$  and  $d_{i\sigma}^+, d_{i\sigma}$  are the creation and annihilation operators of the itinerant electrons in the  $d$ -band Wannier state at site  $i$ .

The first term of (1) is the kinetic energy corresponding to quantum-mechanical hopping of the itinerant  $d$  electrons between sites  $i$  and  $j$ . These intersite hopping transitions are described by the matrix elements  $t_{ij}$ , which are  $-t$  if  $i$  and  $j$  are the nearest neighbours and zero otherwise (in the following all parameters are measured in units of  $t$ ). The second term represents the on-site Coulomb interaction between the  $d$ -band electrons with density  $n_d = N_d/L = \frac{1}{L} \sum_{i\sigma} d_{i\sigma}^+ d_{i\sigma}$  and the localized  $f$  electrons with density  $n_f = N_f/L = \frac{1}{L} \sum_{i\sigma} f_{i\sigma}^+ f_{i\sigma}$ , where  $L$  is the number of lattice sites. The third term is the above mentioned anisotropic, spin-dependent local interaction of the Ising type between the localized and itinerant electrons that reflects

the Hund's rule force. Moreover, it is assumed that the on-site Coulomb interaction between  $f$  electrons is infinite and so the double occupancy of  $f$  orbitals is forbidden.

Since the  $f$ -electron occupation number  $f_{i\sigma}^+ f_{i\sigma}$  of each site  $i$  still commutes with the Hamiltonian (1), the  $f$ -electron occupation number is a good quantum number, taking only two values:  $w_{i\sigma} = 1$  or  $0$ , according to whether or not the site  $i$  is occupied by the localized  $f$  electron. Now the Hamiltonian (1) can be written as

$$H = \sum_{ij\sigma} h_{ij} d_{i\sigma}^+ d_{j\sigma}, \quad (2)$$

where  $h_{ij} = t_{ij} + (Uw_i + Jw_{i-\sigma} - Jw_{i\sigma})\delta_{ij}$ . Thus for a given  $f$ -electron configuration  $w = \{w_1, w_2, \dots, w_L\}$ , the Hamiltonian (2) is the second-quantized version of the single-particle Hamiltonian  $h(w)$ , so the investigation of the model (2) is reduced to the investigation of the spectrum of  $h$  for different configurations of  $f$  electrons. This can be performed exactly, over the full set of  $f$ -electron distributions (including their spins), or approximatively, over the reduced set of  $f$ -electron configurations. Here we use a combination of both numerical methods. The same procedure has been used already in our previous paper [9] to study the ground-states of the extended FKM in one dimension. In the mentioned paper we have also presented some preliminary results concerning the ground states of the model in two dimensions. These results revealed that the extended FKM with spin-dependent interaction between  $f$  and  $d$  electrons can describe various types of charge and magnetic superstructures. In the present paper we try to construct the comprehensive phase diagram (in the  $N_f - N_d$  plane) of the extended FKM in two dimensions. We supply our studies by a detailed finite-size scaling analyses in order to minimize the influence of finite-size effects on the ground-state properties of the model. Here we consider only the case of strong Coulomb interactions ( $U = 4$ ), since the one-dimensional studies showed that the influence of the Hubbard interaction (between  $d$  electrons) on ground-states of the model Hamiltonian (2) can be neglected in this limit. At the end of this paper we specify precisely conditions under which this term can be neglected in two dimensions.

## 2 Results and discussion

To construct the comprehensive picture of charge and magnetic ordering in the extended FKM in two dimensions, the complete phase diagram of the model in the

$N_f - N_d$  plane has been calculated point by point for all even number of  $N_f$  and  $N_d$ . Of course, such a procedure demands a considerable amount of CPU time, that imposes severe restrictions on the size of clusters that can be studied numerically ( $L = 8 \times 8$ ). First we have concerned our attention on the problem of charge ordering. In Fig. 1 we present results of our numerical calculations obtained for  $U = 4$  and  $J = 0.5$  in the form of the skeleton phase diagram. One of the most interesting observations is that the phase diagram consists of only a few configuration types, although the total number of possible configurations increases very rapidly with the cluster size  $L$  as  $3^L$ . In particular, we have detected 5 different charge configuration types, and namely: (a) the segregated configurations, where  $f$  electrons clump together, (b) the n-molecular phases, which have been observed only for small  $N_d$  and small  $N_f$ , (c) the axial stripes, (d) the regular phases (stable only in isolated points) and mixtures of regular (usually chessboard) phases and empty/full lattice accompanied by (e) the miscellaneous configurations. The typical examples corresponding to these configuration types are depicted in the lower part of Fig. 1. As one can see the largest stability regions correspond only three configuration types, and namely, the segregated configurations and the axial stripes, which fill the left and right side of the phase diagram and the regular phases/mixtures of regular phases and empty (full) lattice localized at the central part of the skeleton phase diagram. Moreover, it was found that the homogeneous  $f$ -electron distributions ( $f$  electrons are distributed as far away from each other as possible) are the ground states only in the region  $d$  and only in isolated points, while in the rest part of the phase diagram the inhomogeneous distributions (the segregated phases, the axial stripes, the n-molecular phases) are preferred. This result is very valuable since in the past years a strong interest in the experimental and theoretical studies of strongly correlated systems was focused on the physics that leads to an inhomogeneous ordering, especially to an inhomogeneous charge stripe order due to the observation of such ordering in doped niclate and cuprate materials some of which exhibit high-temperature superconductivity. From the theoretical point of view, the presented skeleton phase diagram clearly demonstrates that this relatively simple model (generalized two-dimensional FKM) can describe such inhomogeneous stripe ordering. Moreover, it was shown that the stability area of stripes is relatively large and, in addition, includes both

physically interesting conditions  $N_f + N_d = L$  and  $N_f + N_d = 2L$ .

Let us now turn our attention on the second problem, and namely, the problem of spin ordering. We have found, that although the charge phase diagram of the generalized two-dimensional FKM is rather simple, the spectrum of magnetic solutions is very rich. As demonstrated in Fig. 2, the one charge distribution could have many different spin configurations and therefore the exact classification is very difficult. Moreover, in the two-dimensional case the finite size effects on spin orderings are still large for clusters with  $L \leq 64$ , and thus we were not able to construct definitive picture of magnetic phase diagram for all  $N_f$  and  $N_d$ . For this reason we have focused our attention on the physically the most interesting cases mentioned above, and namely,  $N_f + N_d = L$  and  $N_f + N_d = 2L$ , where exhaustive studies have been performed. To minimize the finite size effects we have studied the set of finite clusters of  $L = 6 \times 6, 8 \times 8, 10 \times 10, 12 \times 12, 16 \times 16, 18 \times 18$  and  $20 \times 20$  sites.

We have started our study with the case  $N_f + N_d = 2L$ , which is slightly simple for a description. As shown in Fig. 3 the ground states for  $N_f + N_d = 2L$  are antiferromagnetic (AF) with alternating pattern, where the electrons (for  $n_f < 1/2$ ) or holes (for  $n_f > 1/2$ ) form the axial distributions. Our calculations showed that these inhomogeneous stripe distributions are stable for large Coulomb interactions, while decreasing  $U$  leads to their destruction and prefers the homogeneous electron arrangement (see Fig. 4).

From the skeleton phase diagram we know that the condition line  $N_f + N_d = L$  lies in the axial stripe area, but in comparison with the previous case the situation is fully different. The first fundamental difference is that for sufficiently small  $f$ -electron concentrations  $n_f$  the ground state could be ferromagnetically (F) ordered (see Fig. 5). The second one is, that although with increasing  $f$ -electron concentration the ground states are the AF, these AF arrangements are formed by F ordered clusters (domains). In addition, for  $n_f = 1/4$  and  $n_f = 1/3$  ( $L \geq 144$ ) a new type of stripes (known as the ladders) is occurred. And finally, a detailed analyses showed that there exists a critical  $f$ -electron concentration  $n_f^c \sim 1/4$  bellow which the ground-states are phase separated.

To verify the ability of our method to describe ground-state properties of macroscopic systems we have performed similar calculations for  $U = 8$  and several values

of  $n_f$  and  $n_d$  ( $n_f = 3/4, n_d = 1/2$ ;  $n_f = 2/3, n_d = 2/3$ ;  $n_f = 1/2, n_d = 1$ ;  $n_f = 1/3, n_d = 4/3$ ;  $n_f = 1/4, n_d = 3/2$ ) for which there exist the numerical results obtained in the thermodynamic limit ( $L \rightarrow \infty$ ) using the method of restricted phase diagrams [8]. The numerical results for ground-state configurations obtained by these two different approaches are compared in Fig. 6. It is seen that both methods yield the same results for the charge distributions of  $f$ -electrons, but differ in a prediction of spin distributions. To check the stability of our solutions we have performed numerical calculations also for  $L = 12 \times 12, 16 \times 16$  and  $18 \times 18$  clusters. The results obtained are shown in Fig. 7 and they clearly demonstrate that ground states found for  $L = 8 \times 8$  cluster hold also on much higher clusters. This fact allows us to extrapolate our numerical results to the thermodynamic limit, where they can be directly compared with the Lemanski's results. This comparison shows (see Fig. 8) that our method yields in all cases the lower energy in the thermodynamic limit ( $L \rightarrow \infty$ ) than the Lemanski's approach. Moreover, a comparison of our and Lemanski's ground states (Fig. 6) provides a direct explanation of this discrepancy, and namely, that the unit cells used in Ref. [8] are too small to describe correctly the spin distributions.

Although we have presented here only the basic types of charge and magnetic superstructures they clearly demonstrate an ability of the model to describe different types of charge and magnetic ordering. This opens an alternative route for understanding of formation an inhomogeneous charge/magnetic order in strongly correlated electron systems. In comparison to previous studies of this phenomenon based on the Hubbard [10] and  $t - J$  model [11], the study within the generalized spin-one-half FKM has one essential advantage and namely that it can be performed in a controllable way (due to the condition  $[f_{i\sigma}^+ f_{i\sigma}, H] = 0$ ), and in addition it allows easily to incorporate and examine effects of various factors (e.g., an external magnetic field, nonlocal interactions, etc.) on formation of charge and magnetic superstructures.

Of course, one can ask if these results persist also in the more realistic situations when additional interaction terms are included into the Hamiltonian (2). From the major interaction terms that come into account for the interacting  $d$  and  $f$  electron subsystems only the Hubbard type interaction  $U_{dd} \sum_i d_{i\uparrow}^+ d_{i\uparrow} d_{i\downarrow}^+ d_{i\downarrow}$  between the spin-up and spin-down  $d$  electrons has been omitted in the Hamiltonian (2).

In work [8] Lemanski presents a simple justification for the omission of this term, based on an intuitive argument: the longer time electrons occupy the same site, the more important becomes interaction between them. According to this rule the interaction between the itinerant  $d$  electrons ( $U_{dd}$ ) is smaller than the interaction between the localized  $f$  electrons ( $U_{ff}$ ) as well as smaller than the spin-independent interaction between the localized and itinerant electrons. Here we specify more precisely conditions when this term can be neglected. To determine the effects of  $U_{dd}$  interaction on the ground-states of the spin-one-half FKM with spin-dependent interaction ( $J = 0.5$ ) in two-dimensions the exhaustive studies of the ground-state phase diagram of the model (in the  $n_f - U_{dd}$  plane) have been performed. Of course, an inclusion of the  $U_{dd}$  term makes the Hamiltonian (2) intractable by methods used for the conventional spin-one-half/spinless FKM and thus it was necessary to use other numerical methods. Here we used the Lanczos method [12] to study exactly the ground states of the spin-one-half FKM generalized with  $U_{dd}$  interaction between the spin-up and spin-down  $d$  electrons. Such a procedure demands in practice a considerable amount of CPU time, which imposes severe restrictions on the size of clusters that can be studied within the exact-diagonalization method. For this reason we were able to investigate exactly only the clusters up to  $L = 10$ . The results of numerical calculations obtained for  $U = 4$  are summarized in Fig. 9 in the form of  $n_f - U_{dd}$  phase diagram (the half-filled band case  $n_f + n_d = 1$  is considered). One can see that the ground-state configuration  $w^0(N_f)$  found for  $U_{dd} = 0$  persists as a ground state up to relatively large values of  $U_{dd}$  ( $U_{dd}^c \sim 3.5$ ), revealing small effects of the  $U_{dd}$  term on the ground states of the model in the strong  $U$  interaction limit. For this reason our numerical calculations have been done exclusively for large  $U$ .

In conclusion, we have used a combination of small-cluster exact diagonalization calculations and a well-controlled numerical method to study the ground-state properties of the spin-one-half FKM extended by spin-dependent on-site interaction between localized and itinerant electrons in two dimensions. The results obtained have been used to construct the comprehensive picture of charge and spin ordering in this model. It was shown that only a few configuration types form the basic structure of the charge phase diagram in the  $N_f - N_d$  plane. In particular, the largest regions of stability correspond to the phase segregated configurations, the

axial striped configurations and configurations that can be considered as mixtures of chessboard configurations and the full (empty) lattice. Moreover, it was found that the model exhibits a rich spectrum of magnetic solutions including various types of ferro- and antiferromagnetically ordered phases.

This work was supported by Slovak Grant Agency VEGA under Grant No.2/7057/27 and Slovak Research and Development Agency (APVV) under Grant LPP-0047-06. H.C. acknowledges support of Stefan Schwartz Foundation.

## References

- [1] C. H. Chen, S.-W. Cheong, and A. S. Cooper, Phys. Rev. Lett. **71**, 2461 (1993); J. M. Tranquada, D. J. Buttrey, V. Sachan, J. E. Lorenzo, Phys. Rev. Lett. **73**, 1003 (1994); Phys. Rev. B **52**, 3581 (1995); V. Sachan, D. J. Buttrey, J. M. Tranquada, J. E. Lorenzo, G. Shirane, Phys. Rev. B **51**, 12742 (1995).
- [2] J. M. Tranquada, B. J. Sternlieb, J. D. Axe, Y. Nakamura, S. Uchida, Nature (London) **375**, 561 (1995); Phys. Rev. B **54**, 7489 (1996); Phys. Rev. Lett. **78**, 338 (1997); H. A. Mook, P. Dai, and F. Dogan, Phys. Rev. Lett. **88**, 097004 (2002).
- [3] I. Terasaki, Y. Sasago, and K. Uchinokura, Phys. Rev. B **56**, R12685 (1997); K. Takada, H. Sakurai, E. Takayama-Muromachi, F. Izumi, R. Dilanian, and T. Sasaki, Nature (London) **422**, 53 (2003).
- [4] L. M. Falicov, J. C. Kimball, Phys. Rev. Lett. **22**, 997 (1969).
- [5] R. Lemanski, J. K. Freericks, G. Banach, Phys. Rev. Lett. **89**, 196403 (2002); J. Stat. Phys. **116**, 699 (2004).
- [6] P. Farkašovský, H. Čenčariková, and N. Tomašovičová, Eur. Phys. J. B **45**, 479 (2005).
- [7] Y. Ando, K. Segawa, S. Komiyama, and A. N. Lavrov, Phys. Rev. Lett. **88**, 137005 (2002); C. Howald, H. Eisaki, N. Kaneko, M. Greven, and A. Kapitulnik, Phys. Rev. B **67**, 014533 (2003).

- [8] R. Lemanski, Phys. Rev. B **71**, 035107 (2005).
- [9] P. Farkašovský, H. Čenčariková, Eur. Phys. J. B **47**, 517 (2005).
- [10] A. M. Oles, Acta Physica Polonica B **31**, 2963 (2000); J. Frohlich, D. Ueltschi, J. Stat. Phys. **118**, 973 (2005).
- [11] V. J. Emery, S. A. Kivelson, H. Q. Lin, Phys. Rev. Lett. **64**, 475 (1990); L. P. Pryadko, S. A. Kivelson, D. W. Hone, Phys. Rev. Lett. **80**, 5651 (1998); S. R. White, D. J. Scalapino, Phys. Rev. Lett. **80**, 1272 (1998); Phys. Rev. Lett. **81**, 3227 (1998); Phys. Rev. B **60**, R753 (1999); Phys. Rev. B **61**, 6320 (2000).
- [12] E. Dagotto, Rev. Mod. Phys. **66**, 763 (1994).

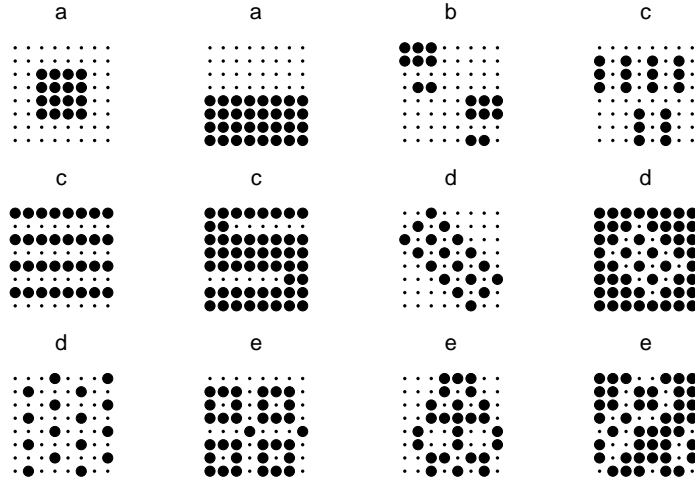
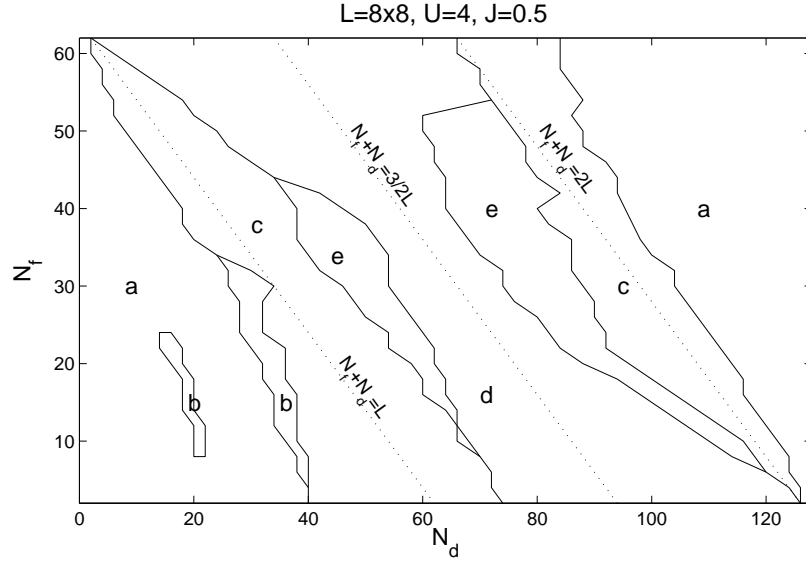


Figure 1: The skeleton phase diagram of the two-dimensional spin-one-half FKM extended by spin-dependent interaction calculated for  $L = 8 \times 8$ ,  $U = 4$  and  $J = 0.5$ . (a) The segregated configurations, (b) the n-molecular phases, (c) the axial stripes, (d) the regular phases, the mixtures of regular phases and full/empty lattice and (e) the miscellaneous phases. Lower part: the typical examples of ground states of the model. Large dots: sites occupied by  $f$  electrons, small dots: vacant sites.

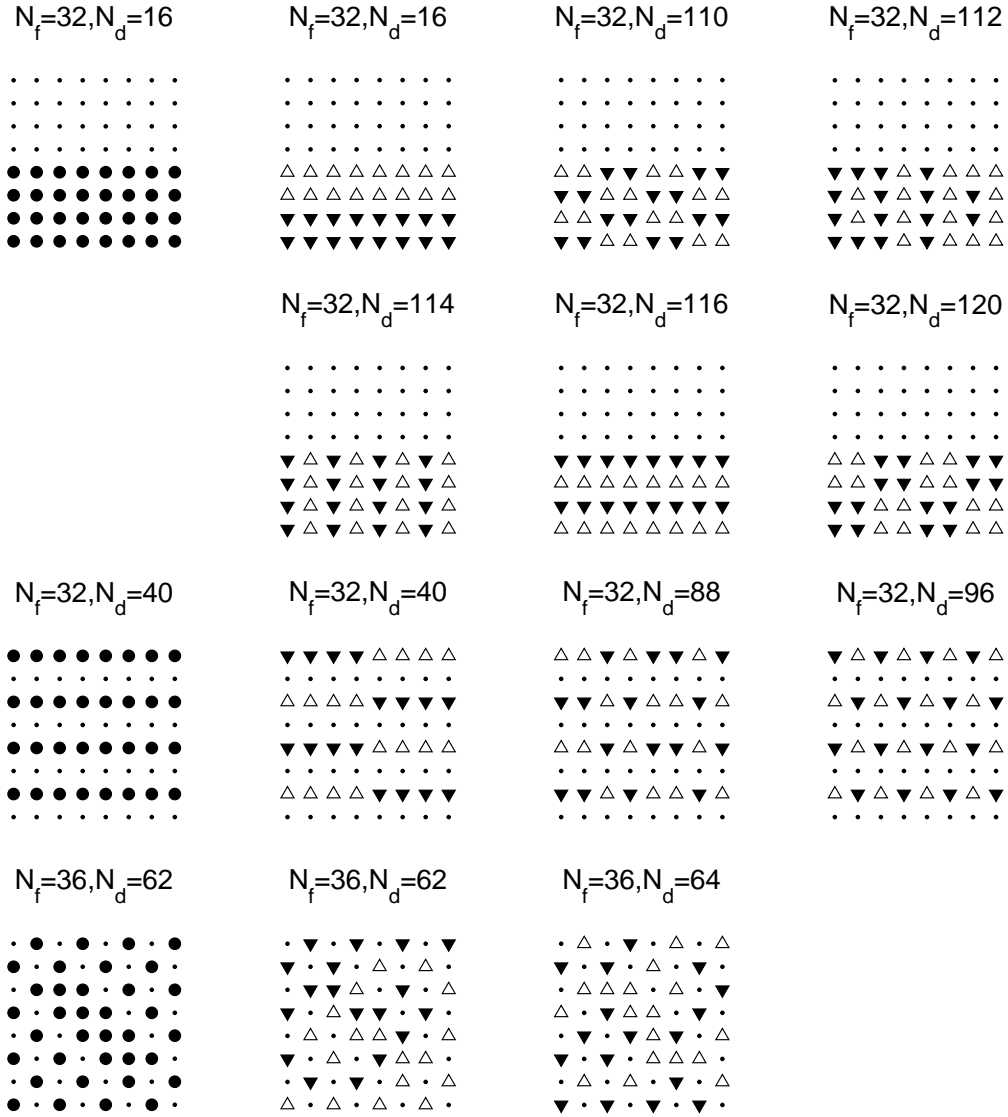


Figure 2: Several spin distributions with common charge pattern depicted on  $L = 8 \times 8$  cluster. To visualize spin distributions we use  $\Delta$  for the up spin electrons and  $\nabla$  for the down spin electrons.

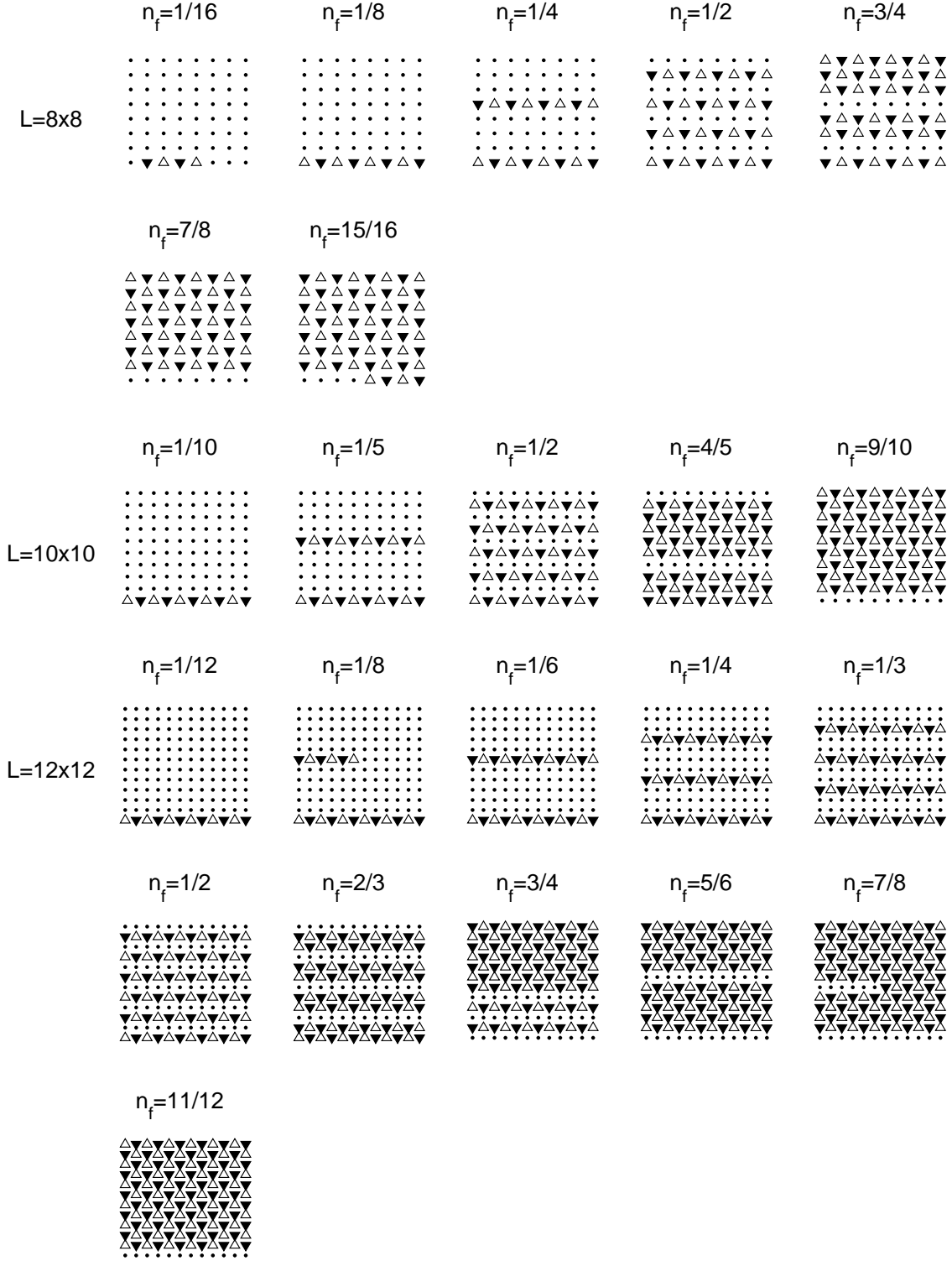


Figure 3: Typical ground-state configurations of the two-dimensional generalized FKM obtained for selected values of  $n_f$  on finite clusters of  $L = 8 \times 8$ ,  $L = 10 \times 10$  and  $L = 12 \times 12$  sites at  $U = 4$ ,  $J = 0.5$  and  $n_f + n_d = 2$ .

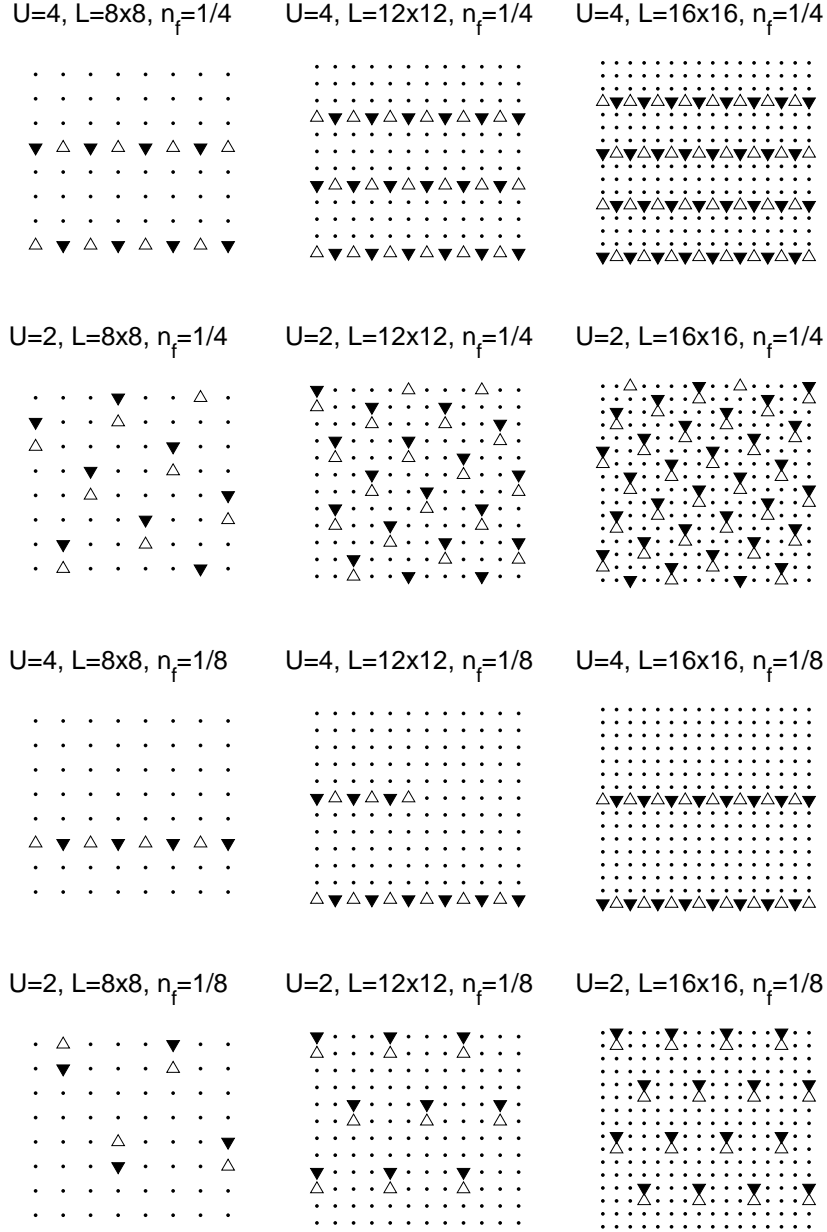


Figure 4: Ground-state configurations of the two-dimensional generalized FKM obtained for different  $U$  ( $U = 4$  and  $U = 2$ ) and  $n_f$  ( $n_f = 1/4$ ,  $n_f = 1/8$  at  $n_f + n_d = 2$ ).

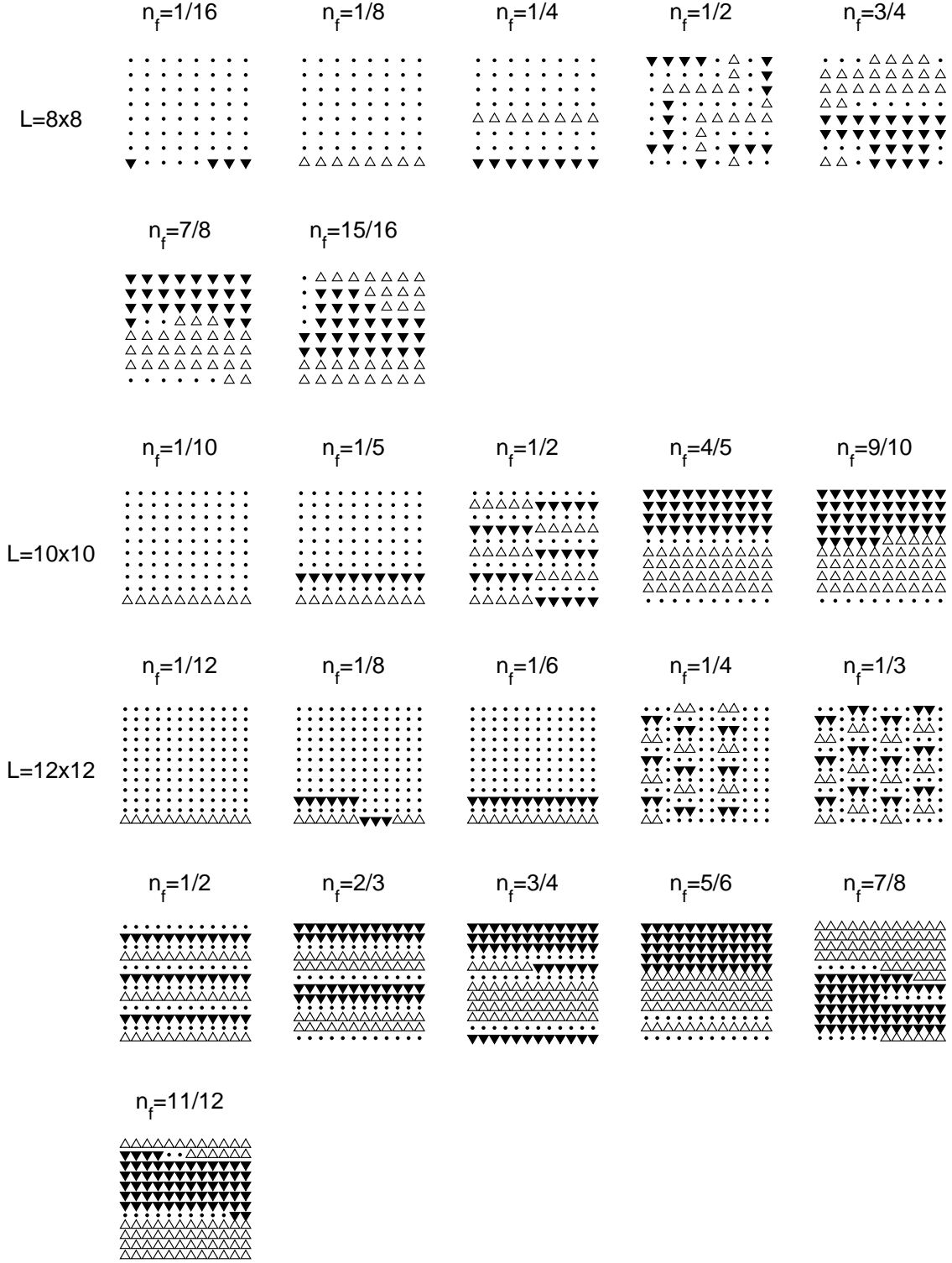


Figure 5: Typical ground-state configurations of the two-dimensional generalized FKM obtained for selected values of  $n_f$  on finite clusters of  $L = 8 \times 8$ ,  $L = 10 \times 10$  and  $L = 12 \times 12$  sites at  $U = 4$ ,  $J = 0.5$  and  $n_f + n_d = 1$ .

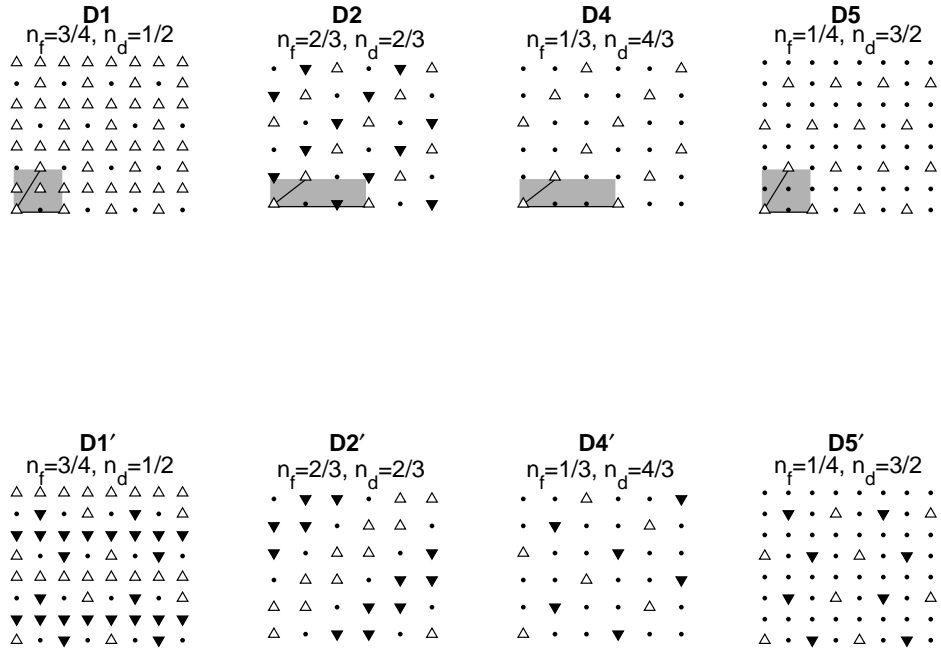


Figure 6: The ground-state configurations of the two-dimensional spin-1/2 FKM for  $U = 8$  and four different pairs of  $n_f$  and  $n_d$  obtained by two different approaches: the method of restricted phase diagrams [8] ( $D1, D2, D4$  and  $D5$ ) and our numerical method ( $D1', D2', D4'$  and  $D5'$ ). The shaded region in the lower left corner shows the unit cell, and line segments show the translation vectors that are used to tile the two-dimensional plane.

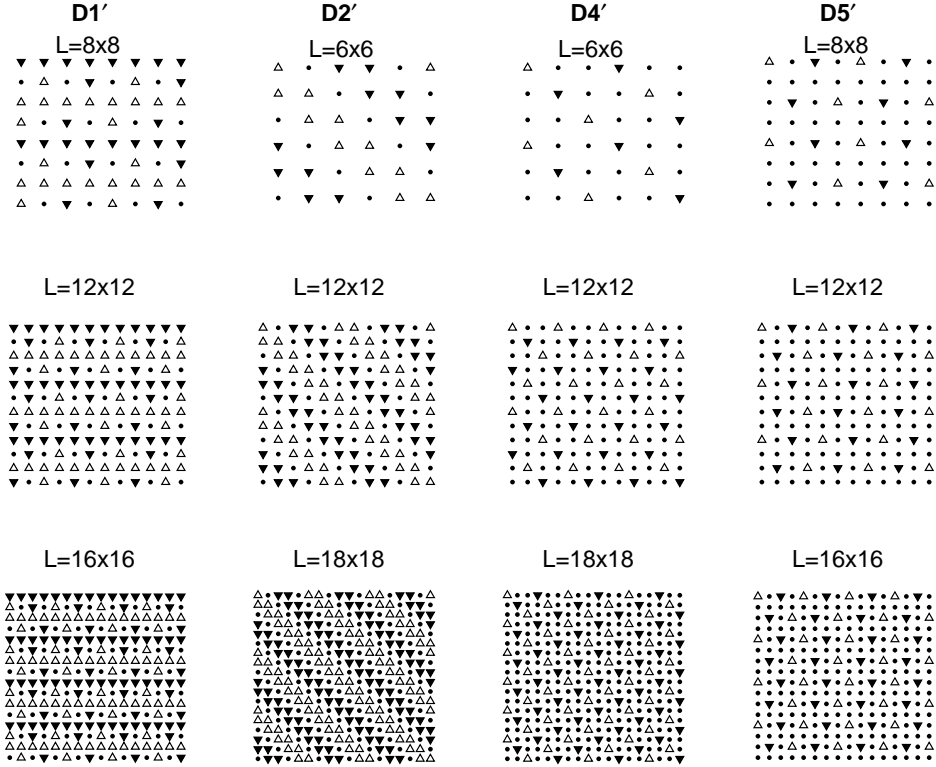


Figure 7: The ground-state configurations of the two-dimensional spin-1/2 FKM calculated for the same  $U, n_f$  and  $n_d$  values as in Fig. 6 on different clusters of  $L = 8 \times 8$ ,  $12 \times 12$  and  $16 \times 16$  sites.

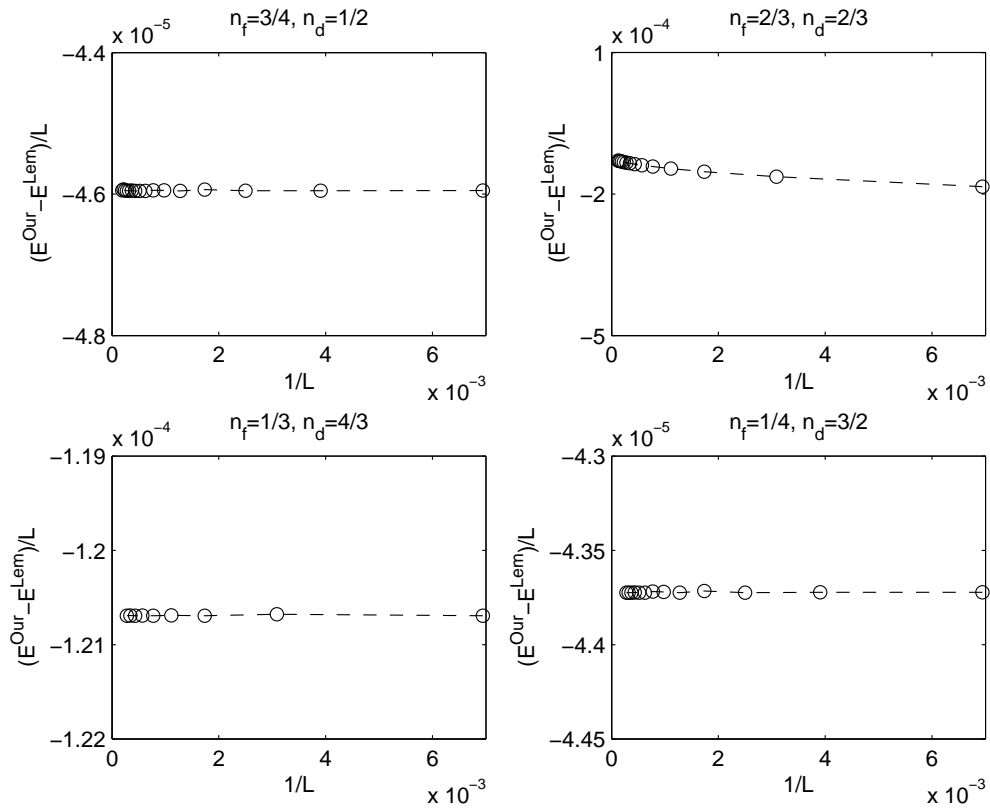


Figure 8: The difference between our and the Lemanski's ground-state energies as a function of  $1/L$  calculated for the extrapolated configurations corresponding to  $D1', D2', D4', D5'$  and  $D1, D2, D4, D5$  phases. The lines are only guides to the eye.

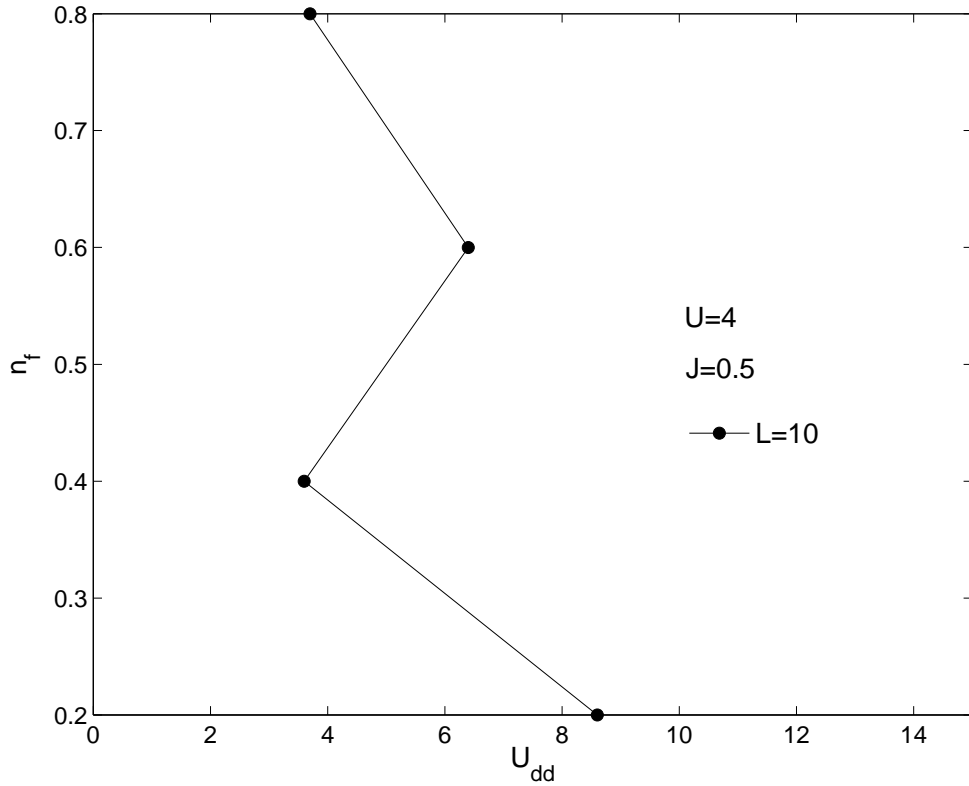


Figure 9: The ground-state phase diagram of the spin-one-half FKM extended by the Hubbard interaction between the itinerant electrons calculated for  $U = 4$  and  $J = 0.5$  on small finite cluster of  $L = 10$  sites. Below  $U_{dd}^c$  the ground states are the ground-state configurations of the conventional spin-one-half FKM ( $U_{dd} = 0$ ). Above  $U_{dd}^c$  these ground states become unstable. The two-dimensional exact diagonalization results.